PROTEINS: Structure, Function, and Genetics 39:47–55 (2000)

Structure and Dynamics of the Pore-Lining Helix of the Nicotinic Receptor: MD Simulations in Water, Lipid Bilayers, and Transbilayer Bundles

Richard J. Law,[1] Lucy R. Forrest,[1] Kishani M. Ranatunga,[1] Paolo La Rocca,[1] D. Peter Tieleman,[2] and Mark S.P. Sansom[1]*

[1]*Laboratory of Molecular Biophysics, Department of Biochemistry, University of Oxford, Oxford, United Kingdom*
[2]*BIOSON Research Institute and Department of Biophysical Chemistry, University of Groningen, Groningen, The Netherlands*

ABSTRACT **Multiple nanosecond duration molecular dynamics simulations on the pore-lining M2 helix of the nicotinic acetylcholine receptor reveal how its structure and dynamics change as a function of environment. In water, the M2 helix partially unfolds to form a molecular hinge in the vicinity of a central Leu residue that has been implicated in the mechanism of ion channel gating. In a phospholipid bilayer, either as a single transmembrane helix, or as part of a pentameric helix bundle, the M2 helix shows less flexibility, but still exhibits a kink in the vicinity of the central Leu. The single M2 helix tilts relative to the bilayer normal by 12°, in agreement with recent solid state NMR data (Opella et al., Nat Struct Biol 6:374–379, 1999). The pentameric helix bundle, a model for the pore domain of the nicotinic receptor and for channels formed by M2 peptides in a bilayer, is remarkably stable over a 2-ns MD simulation in a bilayer, provided one adjusts the pK_As of ionizable residues to their calculated values (when taking their environment into account) before starting the simulation. The resultant transbilayer pore shows fluctuations at either mouth which transiently close the channel. Proteins 2000;39:47–55.** © 2000 Wiley-Liss, Inc.

INTRODUCTION

The nicotinic acetylcholine receptor is the best understood member of the superfamily of ligand-gated ion channels that are responsible for synaptic neurotransmission. Cryoelectron microscopy[2,3] and a wide range of mutagenesis and labelling studies[4–6] have established that the transmembrane pore lies in the center of the molecule and is lined by five M2 α-helices, one from each subunit of the $\alpha_2\beta\gamma\delta$ heteropentamer. Molecular modelling studies restrained by cryoelectron microscopy data indicate that the M2 helices are kinked.[7,8] The kink is thought to be in the vicinity of a Leu residue that is conserved between subunits and between nicotinic receptors from different species. This Leu has been suggested to play a role in the gating mechanism of the channel. It is suggested that the helix kink may correspond to a molecular hinge,[3,8] enabling changes in conformation and packing of the M2 helices in response to binding of neurotransmitter and resulting in a switch from a closed (i.e., ion impermeable) to an open (i.e., ion permeable) channel.

The pore-lining M2 helix has also been studied as a synthetic peptide[9] with a sequence corresponding to M2 from the δ-subunit of the *Torpedo* receptor: Gly[1]-Ser-Glu-Lys-Met-Ser-Thr-Ala-Ile-Ser-Val-Leu-Leu[13]-Ala-Gln-Ala-Val-Phe-Leu-Leu-Leu-Thr-Ser-Gln-Arg[25].

(In this numbering scheme, the conserved Leu residue associated with channel gating is Leu-13). This peptide has been shown to form ion channels in lipid bilayers that share several functional properties with the parent channel.[10] Solution NMR studies of M2 peptide bound to detergent micelles suggest that it forms an unkinked α-helix.[1] Solid state NMR studies of the M2 peptide incorporated into phospholipid bilayers[1,11] show that it retains an α-helical conformation, and the helix axis is tilted by ca. 12° relative to the bilayer normal. Molecular modelling studies[1,12,13] show that this tilt angle is consistent with a left-handed pentameric helix bundle. However, to date modelling studies have been performed in the absence of the complex anisotropic environment provided by a lipid bilayer.

Nanosecond molecular dynamics (MD) simulations for membrane proteins in an explicit bilayer plus water environment are now feasible.[14] This approach may be employed to explore the stability of models developed by in vacuo modelling procedures.[15] It may also be used to examine the interactions of single TM helices with a bilayer environment,[16–19] which is of interest in the context of the two-state model of membrane protein folding.[20] Here we describe MD simulations which reveal the structure and dynamics of a nicotinic M2 peptide in three different systems (Fig. 1): (i) in water (M2/water); (ii) spanning a phospholipid bilayer (M2/TM); and (iii) in a pentameric helix bundle inserted into a lipid bilayer ($M2_5$). Thus, we are able to compare the behavior of the M2 helix in an aqueous environment, in a largely hydrophobic environment, and in a complex environment in which different surfaces of the M2 helix are exposed to water, protein, or lipid.

Grant sponsor: The Wellcome Trust.

*Correspondence to: Mark S.P. Sansom, Laboratory of Molecular Biophysics, The Rex Richards Building, Department of Biochemistry, University of Oxford, South Parks Road, Oxford, OX1 3QU, United Kingdom. E-mail: mark@biop.ox.ac.uk

Received 20 May 1999; Accepted 29 October 1999

TABLE I. Summary of Simulations

Simulation system	Number and duration of simulations	Approximate number of atoms
M2/water	5×2 ns	12,000
Randomised M2/water	1×2 ns	12,000
M2/TM	1×4 ns	21,000
$M2_5$—default ionisation states	1×2 ns	21,000
$M2_5$—ionisation states based on calculated pK_As	1×2 ns	21,000

METHODS

M2 Models

Structures of single M2 helices were taken from the ensemble of solution NMR structures of M2 in micelles[1] (PDB code *1a11*). Models of the $M2_5$ helix bundle were generated by restrained in vacuo MD using a simulated annealing (SA-MD) protocol as previously described.[21] (In order to correspond more closely with the electrophysiological studies[10] the helix bundle was built using a shorter version of M2, omitting residues Glu-1 and Ser-2 from the sequence given above.) Briefly, this involves generation of Cα templates for idealized pentameric bundles of α-helices with the helices orientated such that residues Glu-3, Ser-6, and Ser-10 line the central pore. These Cα templates were used in a two stage SA-MD method, using $n-n+4$ distance restraints to maintain α-helical backbone conformations, and inter-helix distance restraints to maintain the integrity of the four-helix bundle. Each run of the SA-MD procedure yielded an ensemble of 25 structures, from which the structure with the highest five-fold symmetry was selected as the starting point for extended MD simulations in a bilayer/water environment.

Setup of Simulation Systems

For M2/water the initial system was generated by placing the M2 helix in a $(4.9\ \text{nm})^3$ box of water and adding a Cl^- ion to maintain neutrality. This yielded a system containing 11,580 atoms. The set-up of the peptide/bilayer/water systems for MD simulations was essentially as described by Tieleman et al.[15,19] M2 models were embedded in a pre-equilibrated lipid bilayer consisting of 128 molecules of 1-palmitoyl-2-oleoyl-*sn*-glycerol-3-phosphatidylcholine (POPC). In the case of a single M2 helix, the initial position relative to the bilayer was determined by a Monte Carlo simulation which used a simple mean field approximation to a bilayer.[22] A hole was generated in the bilayer by removal of a small number of POPC molecules (1 for M2/TM; 18 for $M2_5$) followed by a short MD simulation during which a cylindrical radial force was applied to repel lipid molecules. The single helix or helix bundle was then placed within the hole. Each system was fully solvated with SPC waters and then energy minimized. Cl^- counterions were added in each case by replacing a single water molecule at positions corresponding to lowest Coulombic energy locations of the ion. Each system was once more energy minimized, followed by an MD equilibration stage of 100 ps during which the backbone atoms of the protein were restrained to their initial positions. During this equilibration period, the system box size and density were monitored and were seen to have relaxed after ca. 50 ps. Production runs consisted of a further 2 ns (or more) of *unrestrained* MD. For M2/TM the system contained 20,632 atoms; for $M2_5$, the system contained 20,937 atoms.

MD Simulations

A summary of all of the MD simulations performed is given in Table I. Note that the total simulation time is ca. 20 ns. MD simulations were carried out as described previously,[15,19,23] using periodic boundary and constant pressure conditions. A constant pressure of 1 bar was applied independently in all three directions, using a coupling constant of $\tau_P = 1.0$ ps.[24] Water, lipid, and peptide were coupled separately to a temperature bath[24] at 300 K using a coupling constant $\tau_T = 0.1$ ps. Long-range interactions were dealt with using a twin-range cut-off: 1.0 nm for van der Waals interactions; and 1.7 nm for electrostatic interactions. The timestep was 2 fs using LINCS[25] to constrain bond lengths and the force field was based on GROMOS 87.[26] The SPC water model used[27] has been shown to behave well in simple lipid/water simulations.[28] Also, the lipid parameters give good reproduction of experimental properties of a DPPC bilayer, and have been used in previous MD studies.[15,19,29,30]

pK_A Calculations

The protonation states of ionizable side chains and of the termini of the $M2_5$ bundle were investigated using a protocol for calculating pK_A values of rings of ionizable side chains in ion channel models.[31] First, the M25 bundle model was embedded in a "slab" of overlapping methane atoms, in order to emulate the low dielectric environment of the surrounding lipid bilayer. Then, $\Delta\Delta G_{BORN}$, the contribution to pK_A shift due to the protein and bilayer environment, and $\Delta\Delta G_{BACK}$, the contribution due to interaction of the residue with non-titratable charges, were used to calculate $pK_{A,INTRINSIC}$:

$$pK_{A,INTRINSIC} = pK_{A,MODEL} - \frac{1}{2.303RT}[\Delta\Delta G_{BORN} + \Delta\Delta G_{BACK}]$$

where $pK_{A,MODEL}$ is the pK_A of an isolated amino acid in free solution.Secondly, the $pK_{A,INTRINSIC}$ value was used to calculate the probability of a residue existing in its ionized state, $p(\mathbf{x})$:

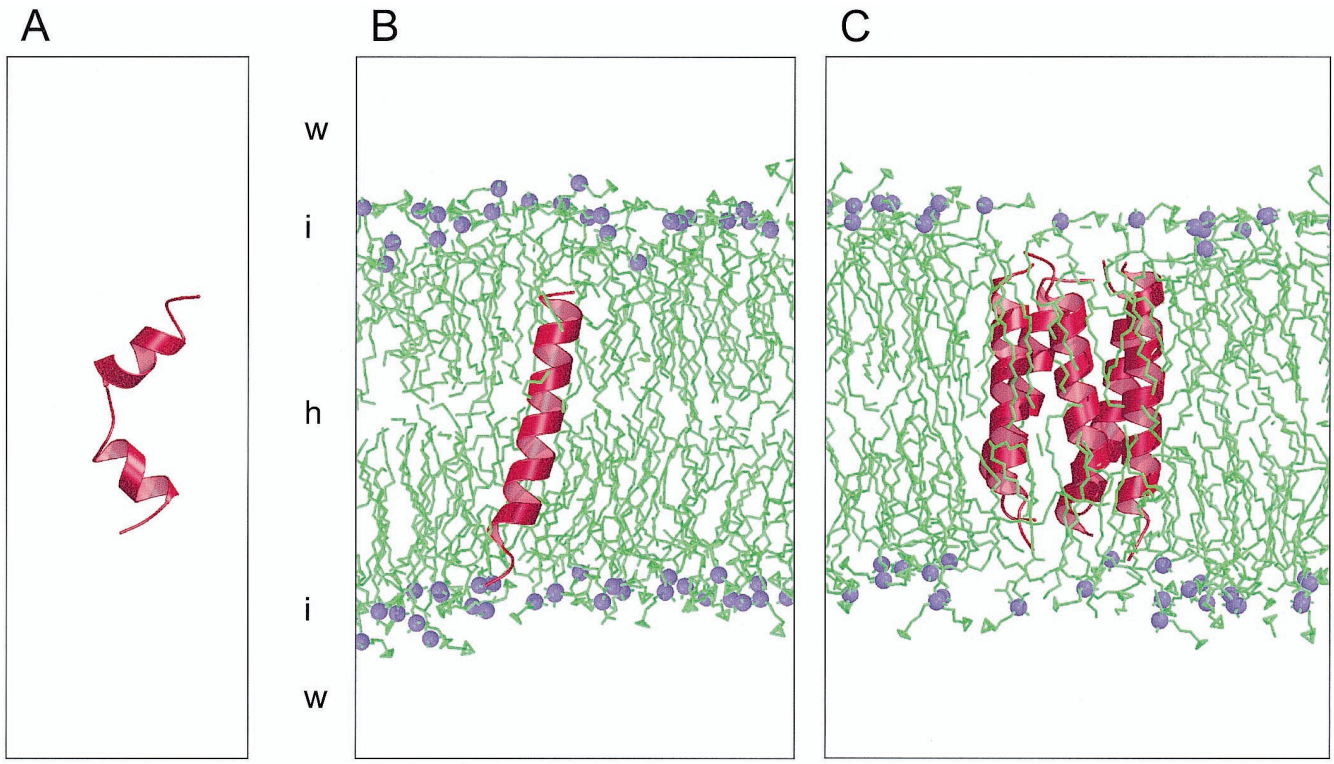

Fig. 1. Snapshots from the three simulation systems. **A:** M2/water; **B:** M2/TM; and **C:** $M2_5$. In each case the structure corresponds to the end of the simulation (i.e., at times 2, 4 and 2 ns respectively). The M2 segment is shown in red, with the C-terminus at the top. In B and C a thin slab through the lipid bilayer is shown, with the POPC molecules in green, apart from the phosphorus atoms which are shown in purple. Water molecules are omitted from all three diagrams, for clarity.

$$p(\mathbf{x}) \propto \exp\left[-\ln 10 \sum_i \gamma_i (pK_{A,INTRINSIC,i} - \mathrm{pH}) - \beta \sum_i \sum_{k<i} \Delta\Delta G_{i,k}\right]$$

where $\beta = RT^{-1}$ and $\mathbf{x}$ is an N-element state vector, whose elements are either 0 or 1 depending on whether the residue is unionized or ionized respectively. $\gamma = -1$ for a basic residue and $\gamma = +1$ for an acidic residue. $\Delta\Delta G_{i,k}$ is the screened Coulombic interaction energy between pairs of ionisable residues i and k. The values of $p(\mathbf{x})$ were used to generate titration curves, from which absolute pK_A values were obtained.

Computational Details

MD simulations were carried out on a 10 processor, 195 MHz R10000 Origin 2000 and on a 72 processor, 195MHz R10000 Origin 2000, and took ca. 8 days per processor per 1ns simulation. Simulations and analysis were carried out using GROMACS (http://rugmd0.chem.rug.nl/~gmx/gmx.html). Electrostatics calculations employed UHBD version 5.1[32] (with some local modifications). Hinge-bending analysis was performed using Dyndom.[33] Pore radius profiles were calculated using HOLE.[34] Other analysis used in-house programs. Initial models were generated using Xplor.[35] Structures were examined using Quanta (Biosym/MSI) and Rasmol, and diagrams drawn using MolScript[36] and Raster3D.[37]

RESULTS AND DISCUSSION

M2 in Water

Simulations of M2 in water have been used to determine whether the helix has an intrinsic propensity for kink formation. Although multi-nanosecond MD simulations are needed to sample fully the unfolding and refolding of peptides in solution,[38] shorter simulations may be used to explore e.g., the first stages of unfolding in water.[19,39] In the NMR structure of M2 peptide in micelles, the helix is unkinked. However, in the cryoelectron microscopy images of the intact receptor protein, a kink is quite evident.[3] Furthermore, cysteine scanning mutagenesis studies suggest a non-α-helical region may be formed in M2 close to Leu-13.[40] Two possible origins of the kink are: (i) the remainder of the receptor protein induces a strain in the M2 segments; and/or (ii) water molecules within the central pore form H-bonds to M2, resulting in local distortion of the helix. In order to define the region most likely to lose α-helical conformation in the presence of water, we ran five 2-ns MD simulations of M2/water. Each simulation started with a different structure from the solution NMR ensemble (pdb code *1a11;*[1]).

Overall progress of the simulations was monitored visually and by following the Cα RMSD from the initial, fully α-helical, structure. The final structure from an M2/water

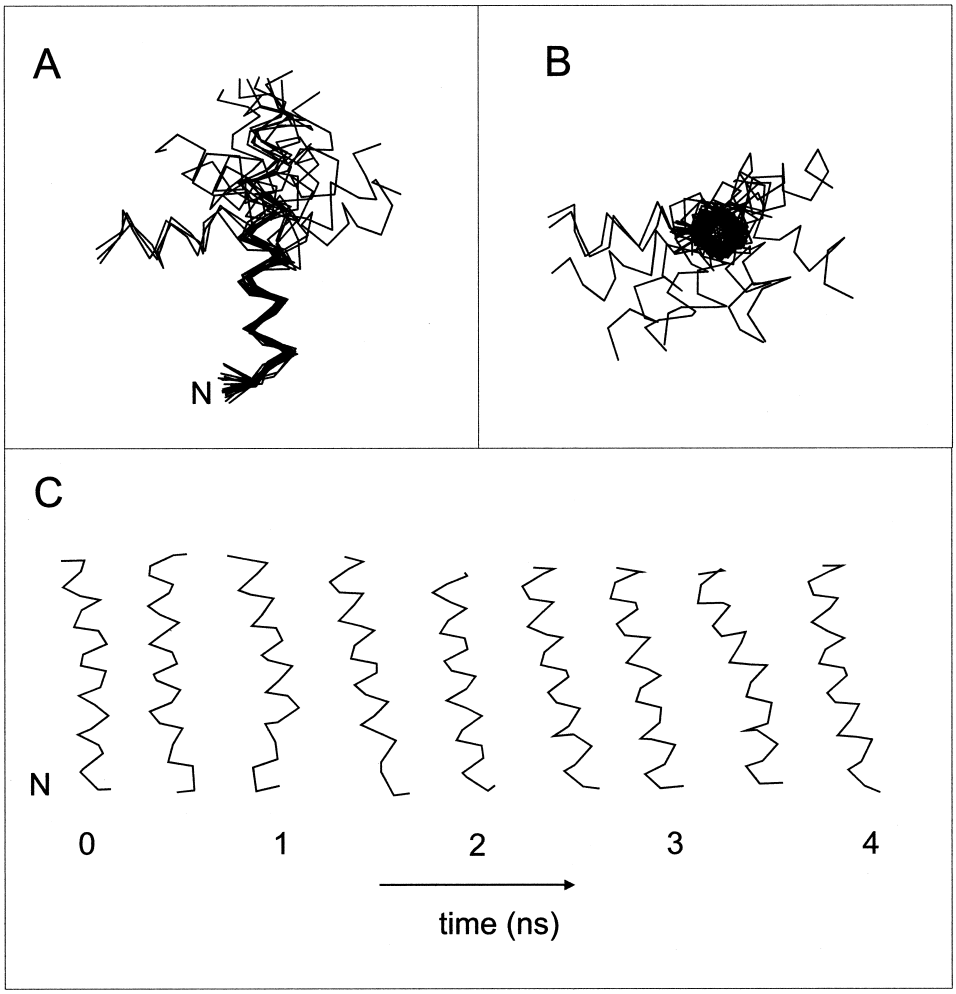

Fig. 2. Successive structures during the **(A,B)** M2/water and **(C)** M2/TM simulations. In A,B Cα traces of structures saved every 100 ps are shown. These are superimposed on the N-terminal α-helical segment (residues 1 to 12) in order to reveal the hinge-bending motion which occurs. The views in A and B are perpendicular to one another. Note that in this diagram the N-terminal helical segments (residue 1–12) are superimposed, and the C-terminal half of M2 is seen to adopt many different orientations. If instead one superimposes the C-terminal half of the molecule then residues 13–25 are seen to form a stable α-helix whilst the N-terminal half adopts many different orientations. C shows Cα traces of M2 from the M2/TM simulation, for structures saved every 0.5 ns. In each case the helix orientation is such that the vertical axis corresponds to the bilayer normal. Thus, the tilt of the helix relative to the bilayer normal can be seen. Note also the small degree of kink of the helix seen in e.g., the 3.5-ns structure.

simulation (Fig. 1A) reveals a major distortion of the M2 helix at the center of the molecule, close to Leu-13. This distortion corresponds to a jump in the Cα RMSD at ca. 800 ps, such that by the end of the simulation the RMSD is ca. 0.45 nm, indicating a major change in conformation from the starting structure.

The helix distortion can be characterized by superimposing successive structures from the simulation (Fig. 2AB). There is evidently a molecular hinge in the vicinity of Leu-13. Motions about this hinge are such that both the helix kink and swivel[41] angles vary as a function of time. The helix kink angle ranges between ca. 0° in the initial structure to ca. 110° at the end of the simulation. However, the kink angle does not increase monotonically but fluctuates during the time course of the simulation, as one might expect for a molecular hinge. The hinge corresponds to local loss of α-helical conformation in the vicinity of Leu-13 (Fig. 3A). This correlates well with the hinge-bending motion identified by Dyndom,[33] which identified Leu-13 as a molecular hinge connecting two rigid helical segments. However, the direction of the bending motion differed between the simulations.

Although 2 ns is a reasonable simulation time by current standards, it is insufficient to fully sample unfolding in water. A number of studies[42] suggest that multiple MD simulations may provide better sampling of conformational space than a single long simulation. We repeated the M2/water simulation five times, each simulation starting with a different M2 structure from the *1a11* NMR ensemble. In four out of five simulations a molecular hinge was formed in the vicinity of Leu-13. A control simulation used an α-helix in which the M2 sequence was randomized (thus mimicking the use of such scrambled peptides in control experiments[1]), to give the sequence: Leu-Met-Ala-Leu-Thr-Ile-Gln-Ser-Arg-Phe-Gln-Ala-Val-Glu-Val-Ser-Leu-Lys-Ser-Leu-Thr-Ser-Leu-Gly-Ala.

The randomized helix unfolded more rapidly than the M2 helix. Unfolding occurred by formation of $i \leftarrow i + 5$ H-bonds at either end of the peptide, a conformation which spread inwards until by 1.9 ns all α-helicity was lost. This pattern of unfolding of α-helices has been seen in simulations of other peptides.[43] Thus, formation of a central molecular hinge can be seen to be a *specific* property of the M2 helix.

These simulations imply that the M2 helix has an inherent tendency, when in an aqueous environment, to form a molecular hinge around Leu-13. This is exactly where a hinge was proposed to exist on the basis of

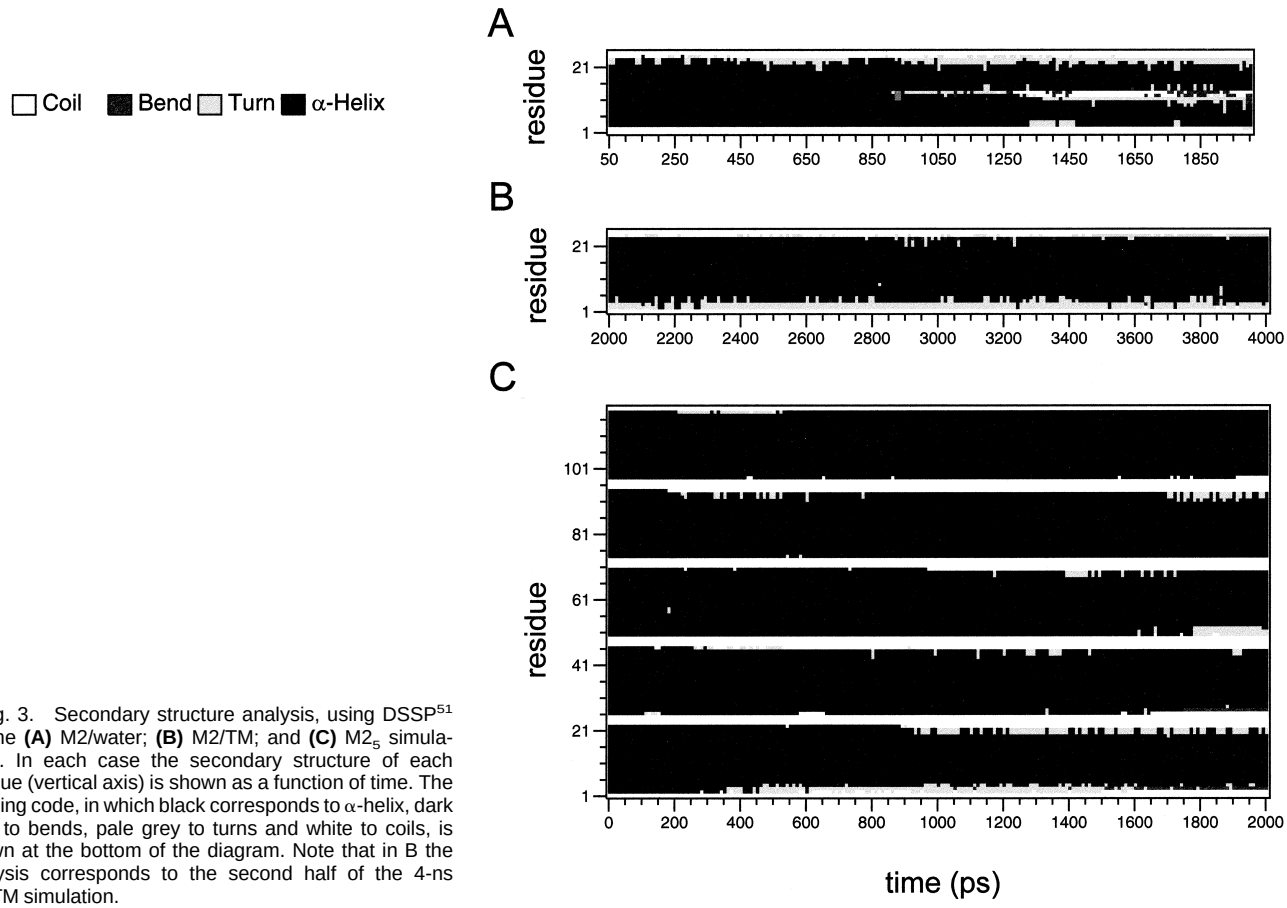

Fig. 3. Secondary structure analysis, using DSSP[51] for the **(A)** M2/water; **(B)** M2/TM; and **(C)** $M2_5$ simulations. In each case the secondary structure of each residue (vertical axis) is shown as a function of time. The shading code, in which black corresponds to α-helix, dark grey to bends, pale grey to turns and white to coils, is shown at the bottom of the diagram. Note that in B the analysis corresponds to the second half of the 4-ns M2/TM simulation.

cryoelectron microscopy and mutagenesis studies.[3] Hinge-formation is correlated with formation of H-bonds between water molecules and the peptide backbone. However, it is conceivable that M2 may have a propensity to kink even when in a hydrophobic environment. Of course, one may ask why M2 is *not* kinked in the NMR structure of the peptide in a micellar environment. This may depend on whether or not the peptide is completely surrounded by detergent molecules, and on what the influence of that detergent is on the conformational dynamics of the helix. We note that, even in somewhat more intensively studied systems such as alamethicin,[44,45] there remains some disagreement between different experimental and computational studies on the exact conformation of the peptide, and simulation studies[19,39] suggest that the conformational dynamics are likely to be modulated by the environment.

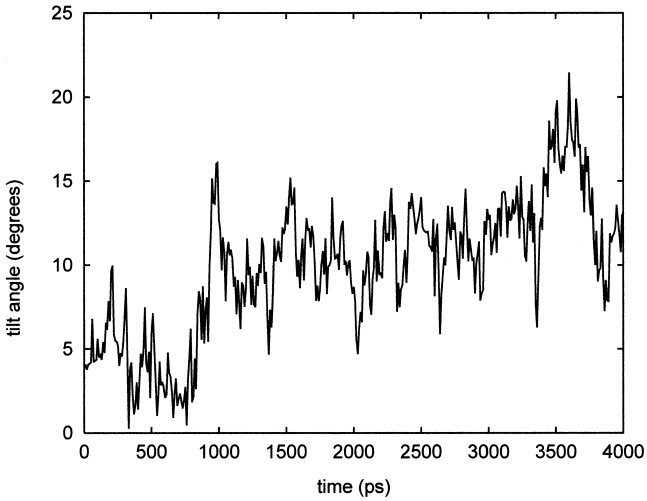

Fig. 4. Helix tilt relative to the bilayer normal as a function for simulation M2/TM. In calculating the helix tilt, the helix axis was defined as a vector from the centre of the Cα atoms of residues 3 to 9 to the center of the Cα atoms of residues 17 to 23.

M2 Spanning a Bilayer

An MD simulation was run, starting with M2 inserted into a POPC bilayer. From the structure at the end of 4 ns (Fig. 1B), it can be seen that M2 spans the hydrophobic core of the bilayer. The apparent mismatch between the helix length and bilayer thickness is compensated for by, *inter alia*, the C-terminal arginine side chain which reaches up to form H-bonds with the headgroup atoms of a lipid molecule. During this simulation the drift of the M2 helix from its initial (NMR; *1a11*) structure is much smaller than in M2/water, giving a final Cα RMSD of ca. 0.1 nm.

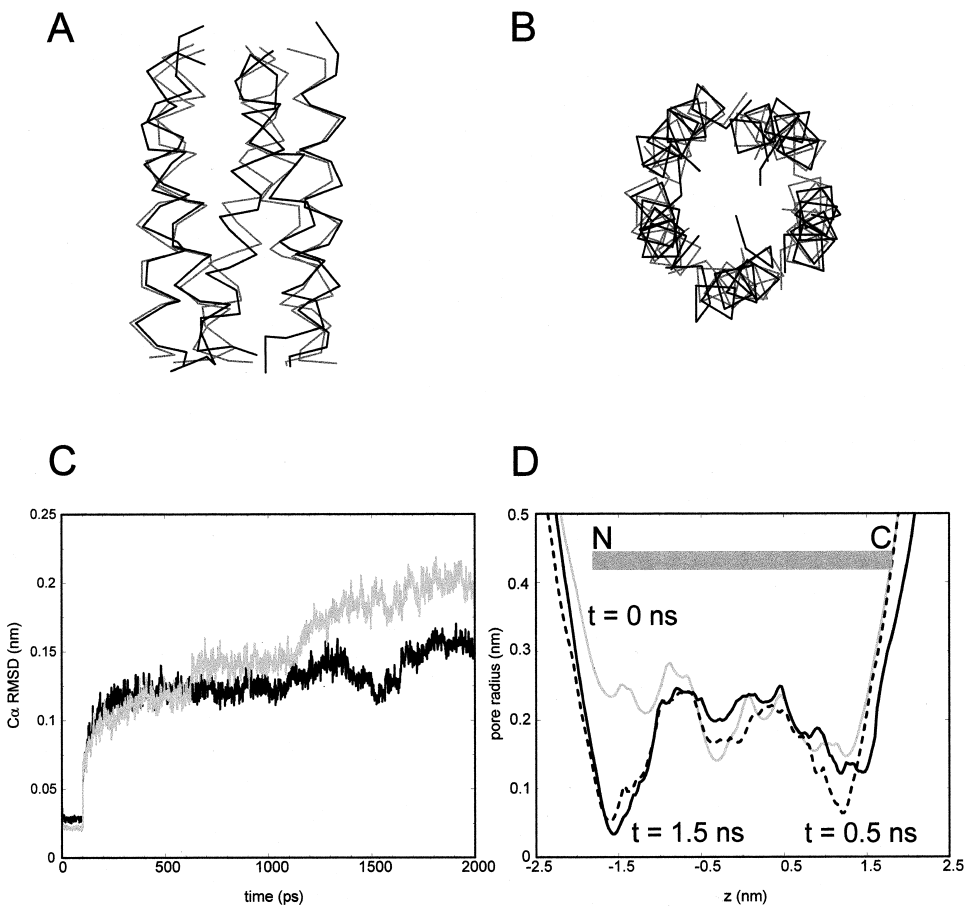

Fig. 5. Simulations of the $M2_5$ helix bundle. **A,B** show superimposed Cα traces of the $M2_5$ helix bundle at the beginning (grey) and end (black) of the 2ns simulation. In **C** the Cα RMSD vs. time (black line) of the $M2_5$ simulation in A,B (in which side chains were adjusted to their predicted ionization states at pH 7) is compared with that for a simulation from the same starting structure in which all residues were assigned their default ionization states (grey line). **D** shows the pore radius profile vs. position along the pore axis. The helix bundle runs from $z = -1.8$ to $z = +1.8$ nm, as indicated by the grey rectangular bar at the top of the diagram. The three curves correspond to the radius profile at $t = 0$ ns (grey line), $t = 0.5$ ns (broken black line) and $t = 1.5$ ns (solid black line).

Thus, at least on a nanosecond timescale, the α-helical conformation of M2 is stable in a transmembrane environment. This was seen in a further four MD simulations, each of 2-ns duration and starting with different members of the NMR ensemble.

The stability of the M2/TM helix can be seen in secondary structure analysis (Fig. 3B). There is just some minor loss of α-helicity at the helix termini. However, successive snapshots of the Cα trace of M2/TM (Fig. 2C) reveal a more interesting picture. Although the α-helix (as defined by DSSP) pattern of H-bonding is not disrupted, there are small but significant deviations from ideal α-helical geometry. In particular there is evidence for transient formation of a kinked helix. This is most evident for e.g., the structure at 3.5 ns, where a kink angle of ca. 20° is observed, the kink being in the vicinity of Leu-13. Thus, although a helix-disrupting molecular hinge is not seen in M2/TM, the M2 segment does not behave as a completely rigid rod even when in a hydrophobic transbilayer environment. In the M2/TM simulation the helix tilts relative to the bilayer normal. The structures in Fig. 3C give a mean (±SD) tilt angle relative to the bilayer normal of 13° (±3°). A more complete analysis is to examine the helix tilt angle as a function of time (Fig. 4). From this, it can be seen that for the first ca. 700 ps the helix is almost parallel to the bilayer normal. The helix then tilts relative to the normal and this orientation is maintained for the remainder of the

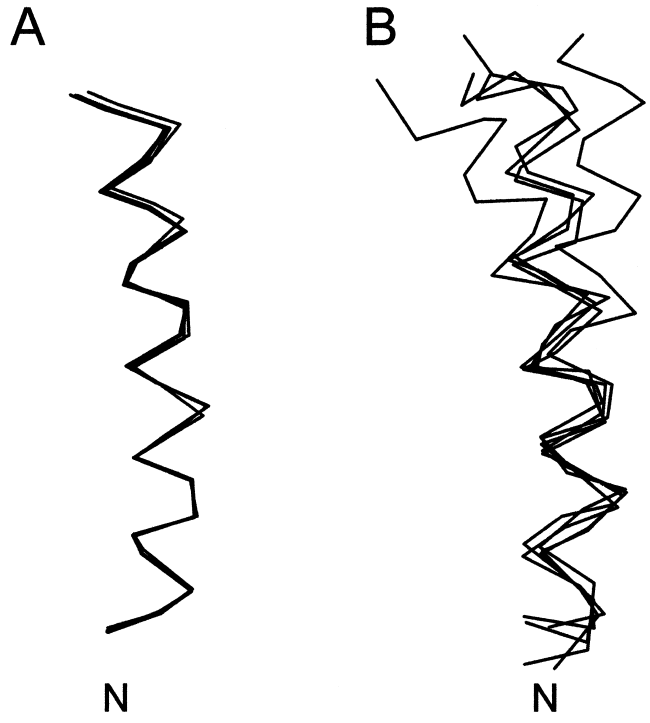

Fig. 6. Superimposed helices from the M25 helix bundle at $t = 0$ ns **(A)** and $t = 2$ ns **(B)**. In each case all five helices of the bundle were superimposed on the Cα atoms of the N-terminal half of the helix.

TABLE II. Isolated Helix in Bilayer Versus Helix Bundle in Bilayer

	Helix 1	Helix 2	Helix 3	Helix 4	Helix 5
Cα-RMSD (2 ns vs. 0 ns)[a] (nm)	0.098	0.113	0.090	0.147	0.070
Cα-RMSD (single TM vs. bundle TM)[b] (nm)	0.216	0.164	0.207	0.223	0.117

[a]Cα RMSD of a TM helix at $t = 2$ns vs. same TM helix at $t = 0$ ns.
[b]Cα RMSD of the single TM helix (at $t = 2$ ns) vs. the five TM helices of the bundle (also at $t = 2$ ns).

simulation. Over the period 1 to 4 ns, the mean (±SD) tilt angle relative to the bilayer normal is 11.5° (±2.9°). This is in good agreement with the solid state NMR data of Opella et al.[1] which gave a tilt angle of 12°. This agreement lends support to the accuracy of the MD simulations. Thus our simulations suggest that the NMR-based picture of the M2 helix is perhaps somewhat static, and may mask transient deviations of bilayer-spanning M2 from ideal α-helical geometry. Of course, it may be that the behavior of the peptide is rather sensitive to the lipid employed. In the solid state NMR studies[1] the lipid used was DMPC. Our simulations POPC which would correspond to a slightly thicker bilayer. Thus, if anything, one might have predicted a smaller tilt and smaller deviations from linearity in our simulations.[46]

$M2_5$ in a Bilayer

The environment of M2 in the intact nicotinic receptor is complex. The pore-lining M2 helices are exposed to water on one face and to (presumably hydrophobic) protein on the other. Thus it is important to examine the structural dynamics of an $M2_5$ bundle as a closer approximation to M2 in the intact channel protein. The simulation started with a model of the $M2_5$ bundle generated by restrained in vacuo MD simulations.[21] In this model the M2 helices were oriented such that polar side chains (Glu-3, Ser-6, and Ser-10), which mutagenesis experiments[4] have identified as pore-lining, pointed towards the center of the bundle. The resultant model had a left-handed supercoil, such that the helices were tilted by ca. 11° relative to the symmetry (i.e., pore) axis.

In setting up the $M2_5$ simulation, predicted pK_A values were used to determine the protonation states of ionizable groups in the bundle. This did not change the protonation states from the neutral pH defaults for any side chains, but did result in protonation of the five C-termini and deprotonation of three of the five N-termini. The importance of this for bundle stability is seen in Fig. 5C. If all groups are assigned their default protonation states, the bundle expands over the 2- ns duration of the simulation (as seen from the radius of gyration vs. time—data not shown) and the bundle structure progressively drifts away from that of the initial model. However, if one takes into account the predicted pK_As, the bundle does not expand significantly and the RMSD, after a rise typical of MD simulations, reaches a plateau of ca. 0.15 nm.

The Cα RMSD (0.15 nm) at the end of the $M2_5$ simulation is quite low, revealing that the initial $M2_5$ bundle model is stable in a bilayer environment, as can also be seen by superimposing the Cα traces of the start and end structures (Fig. 5AB). The helix tilt is unaltered during the course of the simulation, and thus remains consistent with the solid state NMR data of Opella et al.[1] Secondary structure analysis (Fig. 3C) reveals that the five M2 segments remain as α-helices throughout the simulation, apart from minor conformational fluctuations at the helix termini. However, this does not imply that the $M2_5$ bundle is entirely static. In particular, fluctuations at the helix termini alter the radius of the pore running through the center of the bundle. Although the pore is filled with ca. 15 water molecules, the ends of the pore are not always "open" to the bulk water on either side of the membrane. As can be seen from the pore radius profiles (Fig. 5D), fluctuations in the minimum radius at either end of the pore take place on a several hundred ps timescale. Thus, the minimum radius ranges above and below the radius of e.g., a Na^+ ion (ca. 0.095 nm) or a K^+ ion (ca. 0.133 nm). It is tempting to identify such fluctuations with the rapid flickering observed when M2 peptides form ion channels in lipid bilayers.[1] However, the latter fluctuations occur on the msec timescale, rather than the sub-nsec timescale observed in our simulations. Instead, it is possible that rapid fluctuations in channel geometry contribute to the excess electrical noise frequently observed in ionic currents through channels.[47] However, it should be noted that even in the latter case there is a gap of several orders of magnitude between the timescale of the fluctuations observed in the simulation and those inferred from the experimental data.

There is also some evidence for a limited degree of helix kink developing during the $M2_5$ simulation (Fig. 6). The kink angles are similar to those seen in the M2/TM simulation, rather than the pronounced hinge-bending motion in the M2/water simulation. This is despite the exposure of the helices of $M2_5$ to water molecules. It is possible that: (i) packing interactions between neighboring subunits within a bundle restrict possible distortions of the M2 helices; and/or (ii) the alignment of water molecules within the $M2_5$ pore anti-parallel to the helix dipoles (which is observed in the $M2_5$ pore and which has been observed in other pores formed by parallel α-helix bundles[15,48,49]) renders the water molecules less free to form helix distorting H-bonds. However, a comparison of the structures of the single M2/TM helix with the constituent helices of the $M2_5$ bundle (Table II) suggests that the differences in conformation are greater than e.g., the changes in conformation of the bundle helices from start to end of simulation. This suggests that the "mixed" environment provided by the helix bundle may allow somewhat greater flexibility than is possible for the single TM helix.

CONCLUSIONS

The major conclusion of this study is that the pore-lining M2 helix from the nicotinic receptor shows a propensity to kink, and in the presence of water, to form a molecular hinge in the vicinity of Leu-13. This is consistent with a role for kink formation and/or hinge-bending of M2 in the gating mechanism of the nicotinic receptor.[3] However, one must remain cautious in interpreting this result in terms of gating of the receptor per se, because the simulations are on a transmembrane fragment of a much larger receptor protein. However, the two-state model for membrane protein folding[20] does imply that studies of TM helices may be of some relevance to the structure of the intact membrane protein. The secondary conclusion is that MD simulations we have described are capable of reproducing several features of experimental (i.e., NMR) data. In particular, they demonstrate that M2 forms a stable transmembrane helix that adopts the same tilt angle to the bilayer as is seen experimentally. This is encouraging, although it remains uncertain whether the NMR data[1] refer to single M2 helices or to helix bundles spanning a lipid bilayer. Furthermore, in our simulations, the $M2_5$ helix bundle model appears to be stable in a bilayer, at least on a nanosecond timescale. The apparent correlation between the structural properties of M2 in the simulations and in NMR experiments suggests that nanosecond MD simulations can indeed yield accurate information on peptide/bilayer interactions.[50]

ACKNOWLEDGMENTS

LRF is an MRC research student, KMR is a Wellcome Trust research student, and PLR was supported by a BBSRC studentship. DPT was supported by grants from CW/NWO/Unilever. Our thanks to our colleagues for their interest in, and help with, this work. Thanks also to the Oxford Supercomputing Centre for computer time.

REFERENCES

1. Opella SJ, Marassi FM, Gesell JJ, et al. Structures of the M2 channel-lining segments from nicotinic acetylcholine and NMDA receptors by NMR spectroscopy. Nat Struct Biol 1999;6:374–379.
2. Unwin N. Nicotinic acetylcholine receptor at 9Å resolution. J Mol Biol 1993;229:1101–1124.
3. Unwin N. Acetylcholine receptor channel imaged in the open state. Nature 1995;373:37–43.
4. Lester H. The permeation pathway of neurotransmitter-gated ion channels. Ann Rev Biophys Biomol Struct 1992;21:267–292.
5. Changeux JP, Galzi JI, Devillers-Thiéry A, Bertrand D. The functional architecture of the acetylcholine nicotinic receptor explored by affinity labelling and site-directed mutagenesis. Quart Rev Biophys 1992;25:395–432.
6. Hucho F, Tsetlin VI, Machold J. The emerging three-dimensional structure of a receptor: the nicotinic acetylcholine receptor. Eur J Biochem 1996;239:539–557.
7. Sansom MSP, Sankararamakrishnan R, Kerr ID. Modelling membrane proteins using structural restraints. Nat Struct Biol 1995;2: 624–631.
8. Sankararamakrishnan R, Adcock C, Sansom MSP. The pore domain of the nicotinic acetylcholine receptor: molecular modelling and electrostatics. Biophys J 1996;71:1659–1671.
9. Montal M. Design of molecular function: channels of communication. Ann Rev Biophys Biomol Struct 1995;24:31–57.
10. Oiki S, Danho W, Madison V, Montal M. M2δ, a candidate for the structure lining the ionic channel of the nicotinic cholinergic receptor. Proc Natl Acad Sci USA 1988;85:8703–8707.
11. Bechinger B, Kim Y, Chirlian LE, et al. Orientations of amphipathic helical peptides in membrane bilayers determined by solid-state NMR spectroscopy. J Biomol NMR 1991;1:167–173.
12. Montal MO, Iwamoto T, Tomich JM, Montal M. Design, synthesis and functional characterisation of a pentameric channel protein that mimics the presumed pore structure of the nicotinic cholinergic receptor. FEBS Lett 1993;320:261–266.
13. Sankararamakrishnan R, Sansom MSP. Modelling packing interactions in parallel helix bundles: pentameric bundles of nicotinic receptor M2 helices. Biochim Biophys Acta 1995;1239:122–132.
14. Tieleman DP, Berendsen HJC. A molecular dynamics study of the pores formed by *E. coli* OmpF porin in a fully hydrated POPE bilayer. Biophys J 1998;74:2786–2801.
15. Tieleman DP, Berendsen HJC, Sansom MSP. An alamethicin channel in a lipid bilayer: molecular dynamics simulations. Biophys J 1999;76:1757–1769.
16. Woolf TB, Roux B. Structure, energetics, and dynamics of lipid-protein interactions—a molecular-dynamics study of the gramicidin-A channel in a DMPC bilayer. Proteins 1996;24:92–114.
17. Woolf T, Roux B. Structure, energetics, and dynamics of lipid-protein interactions: a molecular dynamics study of the gramicidin A channel in a DMPC bilayer. Proteins 1996;24:92–114.
18. Belohorcova K, Davis JH, Woolf TB, Roux B. Structure and dynamics of an amphiphilic peptide in a lipid bilayer: a molecular dynamics study. Biophys J 1997;73:3039–3055.
19. Tieleman DP, Sansom MSP, Berendsen HJC. Alamethicin helices in a bilayer and in solution: molecular dynamics simulations. Biophys J 1999;76:40–49.
20. Popot JL, Engelman DM. Membrane protein folding and oligomerization: the two-state model. Biochem 1990;29:4031–4037.
21. Kerr ID, Sankararamakrishnan R, Smart OS, Sansom MSP. Parallel helix bundles and ion channels: molecular modelling via simulated annealing and restrained molecular dynamics. Biophys J 1994;67:1501–1515.
22. Gazit E, La Rocca P, Sansom MSP, Shai Y. The structure and organization within the membrane of the helices composing the pore-forming domain of *Bacillus thurigiensis* δ-endotoxin are consistent with an umbrella-like structure of the toxin pores. Proc Natl Acad Sci USA 1998;95:12289–12294.
23. Forrest LR, Tieleman DP, Sansom MSP. Defining the transmembrane helix of M2 protein from influenza A by molecular dynamics simulations in a lipid bilayer. Biophys J 1999;76:1886–1896.
24. Berendsen HJC, Postma JPM, van Gunsteren WF, DiNola A, Haak JR. Molecular dynamics with coupling to an external bath. J Chem Phys 1984;81:3684–3690.
25. Hess B, Bekker H, HJC, BJGEM F. LINCS: a linear constraint solver for molecular simulations. J Comp Chem 1997;18:1463–1472.
26. Hermans J, Berendsen HJC, van Gunsteren WF, Postma JPM. A consistent empirical potential for water-protein interactions. Biopolymers 1984;23:1513–1518.
27. Berendsen HJC, Postma JPM, van Gunsteren WF, Hermans J. Intermolecular Forces. Dordrecht: Reidel; 1981.
28. Tieleman DP, Berendsen HJC. Molecular dynamics simulations of a fully hydrated dipalmitoylphosphatidycholine bilayer with different macroscopic boundary conditions and parameters. J Chem Phys 1996;105:4871–4880.
29. Berger O, Edholm O, Jahnig F. Molecular dynamics simulations of a fluid bilayer of dipalmitoylphosphatidycholine at full hydration, constant pressure and constant temperature. Biophys J 1997;72: 2002–2013.
30. Randa HS, Forrest LR, Voth GA, Sansom MSP. Molecular dynamics of synthetic leucine-serine ion channels in a phospholipid membrane. Biophys J 1999;77:2400–2410.
31. Adcock C, Smith GR, Sansom MSP. Electrostatics and the selectivity of ligand-gated ion channels. Biophys J 1998;75:1211–1222.
32. Davis ME, Madura JD, Luty BA, McCammon JA. Electrostatics and diffusion of molecules in solution: simulations with the University of Houston Brownian dynamics program. Comput Phys Comm 1991;62:187–197.
33. Hayward S, Berendsen HJC. Systematic analysis of domain motions in proteins from conformational change: new results on citrate synthase and T4 lysozyme. Proteins 1998;30:144–154.
34. Smart OS, Goodfellow JM, Wallace BA. The pore dimensions of gramicidin A. Biophys J 1993;65:2455–2460.
35. Brünger AT. X-PLOR version 3.1. A system for X-ray crystallography and NMR. New Haven, CT: Yale University Press; 1992.

36. Kraulis PJ. MOLSCRIPT: a program to produce both detailed and schematic plots of protein structures. J Appl Crystallogr 1991;24: 946–950.
37. Merritt EA, Bacon DJ. Raster3D: photorealistic molecular graphics. Methods Enzymol 1997;277:505–524.
38. Daura X, Jaun B, Seebach D, van Gunsteren WF, Mark AE. Reversible peptide folding in solution by molecular dynamics simulation. J Mol Biol 1998;280:925–932.
39. Tieleman DP, Berendsen HJC, Sansom MSP. Surface binding of alamethicin stabilises its helical structure: molecular dynamics simulations. Biophys J 1999;76:3186–3191.
40. Akabas MH, Kauffmann C, Archdeacon P, Karlin A. Identification of acetylcholine receptor channel-lining residues in the entire M2 segment of the α subunit. Neuron 1994;13:919–927.
41. Sankararamakrishnan R, Vishveshwara S. Geometry of proline-containing alpha-helices in proteins. Int J Pept Protein Res 1992;39:356–363.
42. Caves LSD, Evanseck JD, Karplus M. Locally accessible conformations of proteins: multiple molecular dynamics simulations of crambin. Protein Sci 1998;7:649–666.
43. Kovacs H, Mark AE, Johansson J, van Gunsteren WF. The effect of environment on the stability of an integral membrane helix: molecular dynamics simulations of surfactant protein C in chloroform, methanol and water. J Mol Biol 1995;247:808–822.
44. Sansom MSP. Structure and function of channel-forming peptaibols. Quart Rev Biophys 1993;26:365–421.
45. Cafiso DS. Alamethicin—a peptide model for voltage gating and protein membrane interactions. Ann Rev Biophys Biomol Struct 1994;23:141–165.
46. Killian JA. Hydrophobic mismatch between proteins and lipids in membranes. Biochim Biophys Acta 1998;1376:401–416.
47. Sigworth FJ. Open channel noise 1. Noise in acetylcholine-receptor currents suggests conformational fluctuations. Biophys J 1985;47:709–720.
48. Breed J, Sankararamakrishnan R, Kerr ID, Sansom MSP. Molecular dynamics simulations of water within models of transbilayer pores. Biophys J 1996;70:1643–1661.
49. Mitton P, Sansom MSP. Molecular dynamics simulations of ion channels formed by bundles of amphipathic α-helical peptides. Eur Biophys J 1996;25:139–150.
50. Biggin PC, Sansom MSP. Interactions of α-helices with lipid bilayers: a review of simulation studies. Biophys Chem 1998;76:161–183.
51. Kabsch W, Sander C. Dictionary of protein secondary structure: pattern-recognition of hydrogen-bonded and geometrical features. Biopolymers 1983;22:2577–2637.